# Energy Release Rate Measurement of Welded Bamboo Joints

Haiyang Zhang[1,*], Qian He[1], Xiaoning Lu[1], A. Pizzi[2,3], Changtong Mei[1] and Xianxu Zhan[4]

[1]*College of Materials Science and Technology, Nanjing Forestry University, No. 159 Longpan Road, 210037 Nanjing, China*
[2]*LERMAB, University of Lorraine, 27 rue Philippe Seguin, CS 60036, 88026 Epinal Cedex, France*
[3]*Department of Physics, King Abdulaziz University, Jeddah, Saudi Arabia*
[4]*Dehua Group, Deqing, Zhejiang, China*

**ABSTRACT:** Double cantilever beam tests were used to measure the energy release rates of linear vibrational welded moso bamboo joints. The influence of the length of the preserved cracks, the different combinations of the inner and outer bamboo surfaces and the moisture content is studied herein. The experimental compliance method, which is based on linear elastic fracture mechanics and has been shown to be an ideal method, was used to analyze data with the power equation. The results show that the preserved initial crack length does not have a significant effect on the final measured energy release rate, while the moso bamboo combination does affect the properties dramatically. The welded moso bamboo joints with inner-inner surfaces have the highest energy release rate of 122 J/m$^2$. The average energy release of the outer-outer combination was only 102 J/m$^2$. The expansion of the cracks also became easier when the moisture content of the welded joints was 18.5% compared to 4.5% and 10.1%. So the moisture resistance of the welded joints should be duly improved.

**KEYWORDS:** Energy release rate, welded moso bamboo, moisture content, DCB test

## 1. INTRODUCTION

The expansion of cracks in materials can be studied with fracture mechanics. Energy release rates have been used to quantitatively characterize the formation of the preserved cracks in different kinds of materials [1, 2]. Porter first applied this theory and method to discuss the wood performance [3]. After that, a lot of researchers have used this technique to investigate the crack formation performance of different wood and bonded wood joints. Double cantilever beam (DCB) specimens were employed a lot to study the wood joints in Mode I [4–6]. Long-time studies have shown that it is an available method to study the Mode I fracture performance of the wood adhesive interfaces [7, 8]. The influence of the adhesive type, the relevant polymerization parameters of the adhesives, the wood species and combinations style, the surface performance and the aging process have been explored to identify the source of the different crack formation properties [9]. Various compliance calculation methods such as the ASTM D 3433-75 standard, the direct compliance method, amended foundation beam theory, and Timoshenko beam theory have been chosen to measure the energy release rate of the bonded wood joints with DCB specimens. It has to be shown that the method of experimental compliance is an appropriate approach to evaluate the bonded interface of the wood joints [9].

Linear vibrational wood welding is a new method of bonding wood without the use of the other oil-based additives, but by the wood components themselves. The typical natural, economic, quick and healthy properties have resulted in the wood jointing technique receiving a lot of attention as a promising wood connection method. The assessment of the strength of the welded wood joints has mainly concentrated on the tensile or compression shear test in Mode II [10, 11]. The parameters of the machine sets and many kinds of wood and combinations have been used in this method to optimize properties [12, 13]. The fracture behavior of the welded joints also has to be considered and compared. Especially recently, a growing number of researchers are hoping to use the welding technique to produce wood structure material. Ganne-Chedeville *et al.* first determined the energy release rates of the welded beech joints by DCB specimen and the average energy release rate obtained was 106 J/m$^2$ [14]. And then, the influence of grain orientation both in welding along the wood longitudinal direction and in end-grain-to-end-grain welding were also studied [15]. The results showed that the energy release rates of the welded joints were in the range of

**Corresponding author*: zhanghaiyangnjfu@gmail.com
**DOI: 10.7569/JRM.2017.634180**

the adhesive-bonded joints and sometimes higher than adhesive-bonded joints. Martin Rhême also studied the fracture performance of the welded wood joints under different moisture contents and mode loadings, and then built a finite element model to predict the fracture performance. A satisfactory prediction was received [16, 17].

The objectives of this work were to determine the feasibility of using the double cantilever beam tests to study linear vibrational welded moso bamboo, the influence of the special moso bamboo structure on the energy release rate properties and the effect of moisture content on the crack expansion of the joints.

## 2 EXPERIMENTAL SECTION

### 2.1 Materials

Four-year-old moso bamboo was collected from a bamboo plantation in the Anhui Province of China. The concentration of vascular bundles in the outer zone of the transverse section is very high, reaching 85% and decreasing gradually towards the inner zones, with 45% in the inner part. The ground parenchyma, which is represented by thin-walled cells, surrounds the vascular bundle. The ground parenchyma is very soft while the vascular bundle is very hard. The overall average density of the bamboo is 0.68 g/cm$^3$ with 1.02 ± 0.6 g/cm$^3$ near the outer surface and 0.57 ± 0.5 g/cm$^3$ near the inner surface.

The bamboo was stressed flattened and the flattened bamboo, which came from the same root with a 1–3 m bamboo height, was studied here to eliminate the effect of the performance variation of bamboo. The flattened bamboo was first cut into samples of 250 mm × 20 mm × 8 mm size (L×T×R, the thickness of the moso bamboo used here was about 8 mm) and two of them were linear-vibration welded together to form a joint of 250 mm × 20 mm × (16 ± 1) mm. The samples were welded in the longitudinal-fiber direction. Taking into account the anatomical differences in the transverse section of the bamboo, three series of compositions were achieved: welding of outer and outer faces (O-O), inner and inner faces (I-I) and inner and outer faces (I-O).

### 2.2 Linear Friction Welding

KLN Ultraschall LVW-2261 (Mecasonic, Crest Group, Annemasse, France), which was formerly designed for welding thermoplastics with complete process control, was used here. Its vibration welding frequency was 150 Hz. The whole welding process could be divided into two stages: the main welding phase and the cooling pressure-holding phase. In the cooling pressure-holding phase, there was no friction applied in the samples and the amplitude was zero. The time of the cooling phase was 10 s and the pressure was 2.5 MPa. In order to make the temperature rise smoothly in the welded surfaces, the main welding process was made up of three phases. The first phase was the pressure-increasing phase, so 1 s (time), 0.5 MPa (pressure) and 1 mm (amplitude) were set for this phase. The next two phases mainly decide the final properties of the welded joints and Table 1 shows the different parameters for the machine set which has been optimized [18]. The amplitude was 2 mm and the welding time totaled 5 s and the welding pressure increased to 0.25 MPa, as shown in Table 1. The moisture content of the moso bamboo samples before welding was 11% and the moisture content was constant owing to the fast welding process.

### 2.3 DCB Test and Energy Release Rate Calculation Method

Figure 1 shows the DCB test specimens. Two metal blocks with loading fixture were glued onto the loading place of the sample surface with quick-drying adhesive. The samples were clamped to the Instron mechanical testing machine by the glued metal blocks. A small band saw was used to produce a 1.5 mm wide kerf along the welding interface. The length of the preserved crack along the welded interface was 50 mm, 100 mm, 150 mm and 200 mm. The experiment was repeated 5 times in each group.

Then a white paint was used to cover the welded interface in order to visualize the extension of the preserved crack. The maximum load capacity of the test machine was 10 kN. The loading speed was

**Table 1** Welding parameters for the bamboo joints.

| Groups | Welding parameters | | |
|---|---|---|---|
| | Time (s) | Pressure (MPa) | Amplitude (mm) |
| I-O | 1/2/3/10 | 0.50/1.75/2.00/2.50 | 1/2/2/0 |
| O-O | 1/2/3/10 | 0.50/1.75/2.00/2.50 | 1/2/2/0 |
| I-I | 1/2/3/10 | 0.50/1.50/1.75/2.50 | 1/2/2/0 |


**Figure 1** Double cantilever beam test specimen.


 

1 mm/min. When the loading force decreased quickly, the test was finished. A displacement transducer was used to measure the crack opening process with the loading force. When the preserved crack began to develop, the loading force dropped and the machine stopped the test. Every group had five replications.

Mode I interlaminar fracture energy release rate $G_{IC}$ for DCB specimen according to ASTM D5528 (2001) can be written as:

$$G_{IC} = -\frac{1}{b} \cdot \frac{dU}{da} \tag{1}$$

where *Pc* is the loading force when the crack begins to propagate, *b* is the width of the specimen, *U* is the total strain energy and *a* is the length of the preserved crack.

The total strain energy *U* can be calculated by the loading force:

$$U_{cr} = \frac{1}{2} F_{cr} \delta = \frac{1}{2} F_{cr}^2 C \tag{2}$$

where $F_{cr}$ is the critical loading force and $\delta$ is the displacement resulting from the critical loading force and *C* is the compliance with:

$$C = \frac{\delta}{F_{cr}} \tag{3}$$

And then Mode I interlaminar fracture energy release rate $G_{IC}$ can be written as:

$$G_{IC} = -\frac{1}{b} \cdot \frac{d\left(-\frac{1}{2} F_{cr}^2 C\right)}{da} = \frac{F_{cr}^2}{2b} \cdot \frac{dC}{da} \tag{4}$$

According to the F-$\delta$ curves of the DCB tested specimen, different crack lengths generate different loading procedures. The slope of the curve decreases with the increase of the crack length. The functional relationship between the compliance *C* and the crack length *a* can be established by the fitting method. The power equation was chosen here to build up the relationship:

$$C = qa^m \tag{5}$$

where *q*, *m* are the fitting coefficients of the power equation.

And now the energy release rate $G_{IC}$ can be given and calculated by:

$$G_{IC} = \frac{F_{cr}^2}{2b} \cdot \frac{dC}{da} = \frac{F_{cr}^2}{2b} \times qma^{m-1} \tag{6}$$

**Table 2** Salts used to set the RH in climatic box.

| No. | Salt | RH (%) | MC (%) |
|---|---|---|---|
| 1 | KOH | 9 | 4.5 |
| 2 | $Na_3N$ | 65 | 10.1 |
| 3 | $K_2SO_4$ | 97 | 18.5 |

## 2.4 Moisture Content Modification

Three desiccators with different relative humidity (RH) climates were used to adjust the equilibrium moisture content of the welded samples. The experimental ambient temperature was kept at 20 °C. Saturated salt solution corresponding to different RHs is shown in Table 2. The welded moso bamboo joints which had achieved a stable weight in the different climate boxes had the corresponding moisture content determined by the oven-drying method with 4.5%, 10.1% and 18.5%, respectively. After that, the welded moso samples were done with DCB test methods to study the moisture content on the final fracture energy release rate of the welded joints. The test procedure and calculation methods were all the same as the dry state measurement.

## 2.5 Statistical Analysis

The results of the experiment were analyzed using SPSS 17.0.

# 3 RESULTS AND DISCUSSION

During all DCB testing, there was no R-curve behavior detected. So the fracture process zone could be neglected. Figure 2 shows the typical F-$\delta$ curve with different initial crack length with I-O welded moso bamboo joints. The determinants of the critical loading force $F_{cr}$ and the corresponding displacement $\delta$ are shown in Figure 2. The broken surfaces are displayed in Figure 3, which indicate that the crack expands along the welded interface. There is no visible original bamboo broken after the DCB tests.

Fitting result with the power equation of I-O welded joints is shown in Figure 4. The compliance is calculated with displacement $\delta$ and critical loading force $F_{cr}$ determined in Figure 2 by Equation 3. The compliance used to determine the fitting coefficient is the average of the five results. Table 3 shows all three dry state fitted coefficients by power equation and the results show good correction with coefficient $R^2$ between 0.98–0.99.

Table 4 shows the measured results of $G_{IC}$ with different preserved crack length *a* by three moso bamboo

 

 DOI: 10.7569/JRM.2017.634180

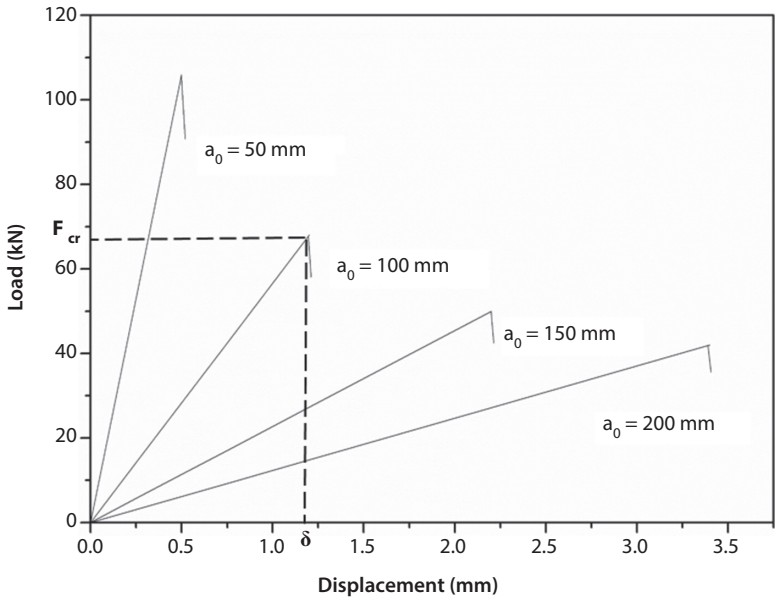


**Figure 2** Typical F-$\delta$ curve with preserved crack length 50 mm, 100 mm, 150 mm and 200 mm of I-O joints and the critical loading force Fcr; the corresponding displacement $\delta$ is marked with a dotted line.

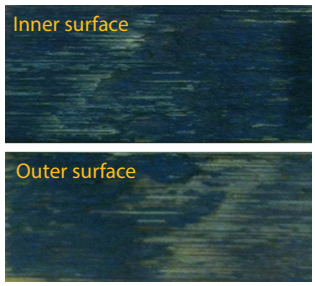


**Figure 3** The broken surface of the welded I-O moso bamboo joints after DCB testing where no obvious broken original bamboo can be seen.

welded combinations. One-way analysis of variance by SPSS Statistics software, 11.5 edition, was used to determine whether the preserved crack length had significant influence on $G_{IC}$. The analysis indicated that P-values are 0.28, 0.06 and 0.84 corresponding to the I-O, O-O and I-I groups respectively. So there were no significant differences in each group measured by different initial crack length *a*. All the data could be used to describe the distributions of the groups. And all the cracks were found to be propagated along the interface between the welded bamboo, no matter what kind of combination there was.

One-way analysis of variance was also used here to study the effect of the welding method on the final $G_{IC}$. P-value with 0.0002 showed that the different welding combinations had significant influence on the measure $G_{IC}$. Every two groups with different combinations were also analyzed with a T-test (Figure 5). The I-I welded moso bamboo joints had the highest average $G_{IC}$ with 122 J/m$^2$, while the O-O welded moso bamboo had the lowest average $G_{IC}$ with 102 J/m$^2$. The average of $G_{IC}$ of the I-O bamboo welded joints was 118 J/m$^2$, which was close to the average I-I $G_{IC}$. But, the variation coefficient of I-O welded joints was 16%, which was greater than the variation coefficient of O-O joints with 9%. The variation coefficient of I-I joints was 11%.

The distribution of the vascular bundles had a great influence on the final performance of the welded bamboo joints. The hard vascular bundles in the bamboo, which could be seen as the natural reinforcement [19, 20], could not be melted and broken in the welding process. The material flow in the welding process was only attributed to the other bamboo cells which had abundant lignin. So the shortage of melted and flowing materials made the final O-O joints very poor. On the contrary, the strength of the I-I welded joint was shown to be higher owing to the flow of melt-rich material.

The influence of the moisture content on the different welded joints is shown in Figure 6. Moisture content had a significant influence on the $G_{IC}$ among the three combinations. Every two groups in each combination were also compared with a T-test for a more precise analysis. The results indicated that the highest MC decreased the final $G_{IC}$ of the welded moso bamboo joints. The rate of average $G_{IC}$ descent of 20% MC was 32%, 30% and 35% compared to 11% MC, respectively. The $G_{IC}$ value of the low MC with 4.5% and 11% MC were very similar and there was no

  

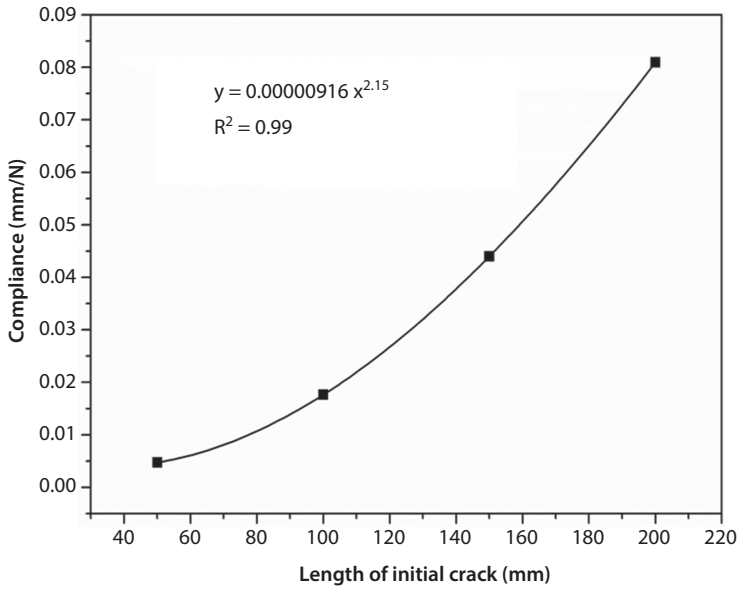


**Figure 4** Fitted curve of the compliance and initial crack length of I-O welded joints with the power equation.

**Table 3** The fitting coefficients determined by the power equation.

| Groups | q | m | $R^2$ |
|---|---|---|---|
| I-O | 0.00000916 | 2.15 | 0.99 |
| O-O | 0.00001213 | 2.21 | 0.98 |
| I-I | 0.00000864 | 2.23 | 0.99 |

**Table 4** Values of the energy release rate measured by different preserved crack length.

| Groups | a (mm) | $G_{IC}$ (J/m²) | | | | |
|---|---|---|---|---|---|---|
| I-O | 50 | 88 | 125 | 99 | 108 | 120 |
| | 100 | 95 | 131 | 127 | 112 | 112 |
| | 150 | 133 | 118 | 126 | 90 | 133 |
| | 200 | 103 | 125 | 140 | 152 | 125 |
| O-O | 50 | 82 | 87 | 95 | 105 | 93 |
| | 100 | 112 | 101 | 112 | 89 | 86 |
| | 150 | 110 | 96 | 111 | 129 | 110 |
| | 200 | 107 | 105 | 101 | 102 | 98 |
| I-I | 50 | 101 | 117 | 143 | 138 | 132 |
| | 100 | 134 | 122 | 110 | 134 | 106 |
| | 150 | 120 | 128 | 134 | 106 | 105 |
| | 200 | 128 | 110 | 119 | 134 | 114 |

statistical difference. As we know, the mechanical performance of the wood is negatively influenced by the MC under the fiber saturation point. The strength of the welded wood joints also decreased upon exposure to water, which has been reported in the literature [21, 22]. Peña *et al.* studied the composition of the welded wood joints and indicated that the welded interface materials could dissolve more in water than the original wood [23]. The friction acts during the welding, which leads to a very moisture-sensitive interface. Under a dry condition with 4.5% or 11% MC, the broken surface after the DCB test showed that the bamboo fibers were contained in the molten matrix. However, the bamboo fibers were found to pull out of the molten materials, which meant the strength of the interface material had been decreased by the high MC. Under these circumstances, there was a big drop of the macro-level $G_{IC}$ value.

## 4 CONCLUSIONS

1. Double cantilever beam test method is a suitable way to measure and compare the fundamental properties of the welded moso bamboo joints with different outer and inner surface combinations. All expansion cracks were located in the interface of the welded line without showing typical R-curve behavior.
2. Preserved initial crack length does not have a significant influence on the final energy release rate of the welded moso bamboo joints, no matter what kind of combination there is in the range of 50 to 200 mm when the total length of the sample is 250 mm. But the distribution of the vascular bundles do have a great effect on the energy release rate of the joints. The O-O welded

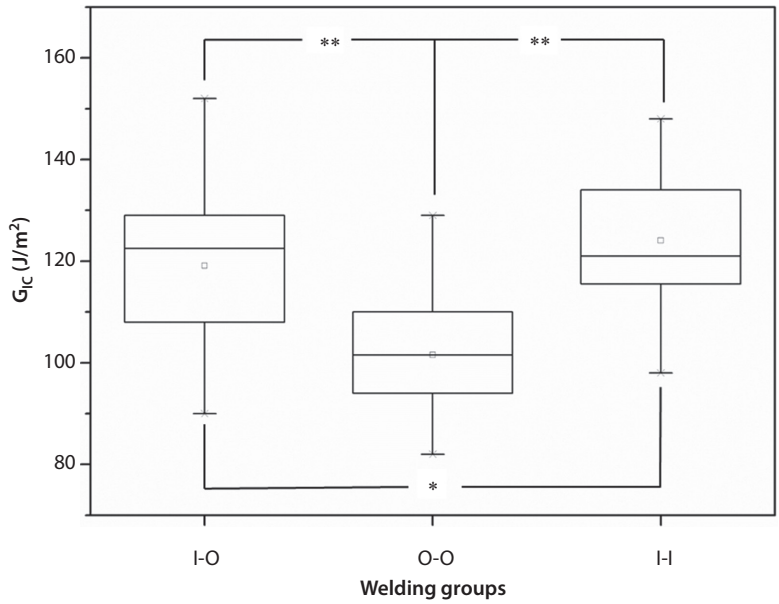


**Figure 5** The energy release rate of the inner-outer, outer-outer and inner-inner welded joints (**: $p < 0.01$, *: $p < 0.05$, N.S. $\geq 0.05$).

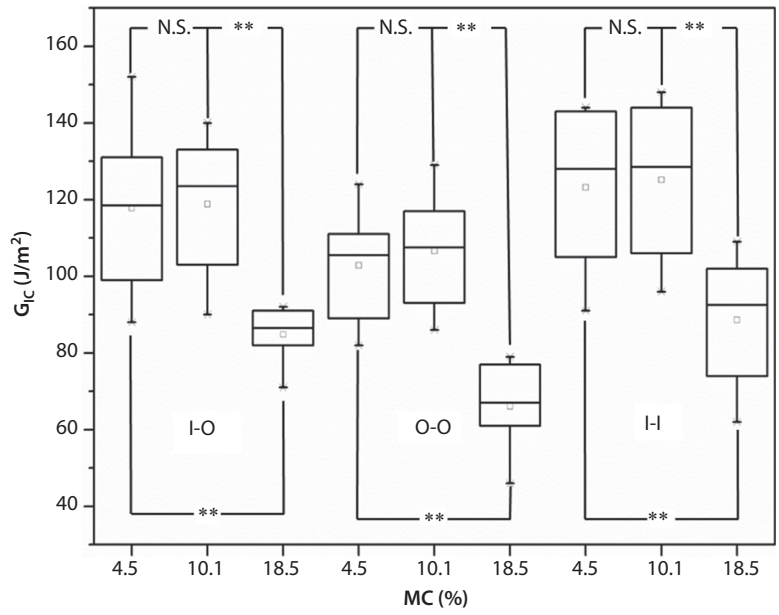


**Figure 6** The influence of the moisture content on the energy release rate of the welded moso bamboo joints (**: $p < 0.01$, *: $p < 0.05$, N.S. $\geq 0.05$).

joints with less vascular bundles showed the highest performance, while the I-I the lowest.

3. Moisture content also determined the crack expansion property of the welded moso bamboo joints. When the moisture content of the samples reached 18.1%, the energy release rate of the welded joints decreased quickly owing to the poor water resistance of the welded interface.

## ACKNOWLEDGMENTS

The authors are grateful for support from the Science and Technology Department of Jiangsu Province under Grant BK20150878, the Nanjing Forestry University under Grant cx201617, and the Priority Academic Program Development of Jiangsu Higher Education Institutions (PAPD).

  

## REFERENCES


1. N. Sela and O. Ishai, Interlaminar fracture toughness and toughening of laminated composite materials: A review. *Composites* **20**, 423–435 (1989).
2. C.A. Papadopoulos, The strain energy release approach for modeling cracks in rotors: A state of the art review. *Mech. Syst. Signal Process.* **22**, 763–789 (2008).
3. A. Porter, On the mechanics of fracture in wood. *Forest Prod. J.* **14**, 325–331 (1964).
4. J.G. Williams, On the calculation of energy release rates for cracked laminates. *Int. J. Fract.* **36**, 101–119 (1988).
5. F.E. Penado, A closed form solution for the energy release rate of the double cantilever beam specimen with an adhesive layer. *J. Compos. Mater.* **27**, 383–407 (1993).
6. K. Shimamoto, Y. Sekiguchi, and C. Sato, Effects of surface treatment on the critical energy release rates of welded joints between glass fiber reinforced polypropylene and a metal. *Int. J. Adhes. Adhes.* **67**, 31–37 (2016).
7. O.R. Shah and M. Tarfaoui, Determination of mode I & II strain energy release rates in composite foam core sandwiches. An experimental study of the composite foam core interfacial fracture resistance. *Compos. Part B: Eng.* **111**, 134–142 (2017).
8. Z. Jiang, S. Wan, M. Li, and L. Ma, Analytical solutions for non-uniformity of energy release rate of orthotropic double cantilever beam specimens with an adhesive layer. *Eng. Fract. Mech.* **164**, 46–59 (2016).
9. B. Xu, Y. Wang, and Y. Zhao, State-of-the-art of wood fracture toughness along the grain. *Mechanics in Engineering* **38**, 493–500 (2016).
10. B. Gfeller, M. Zanetti, M. Properzi, A. Pizzi, F. Pichelin, M. Lehmann, and L. Delmotte, Wood bonding by vibrational welding. *J. Adhes. Sci. Technol.* **17**, 1573–1589 (2003).
11. M. Boonstra, A. Pizzi, C. Ganne-Chedeville, M. Properzi, J.M. Leban, and F. Pichelin, Vibration welding of heat-treated wood. *J. Adhes. Sci. Technol.* **20**, 359–369 (2006).
12. M. Vaziri, O. Lindgren, and A. Pizzi, Optimization of tensile-shear strength for linear welded scots pine. *J. Adhes. Sci. Technol.* **26**, 109–119 (2012).
13. P. Omrani, H.R. Mansouri, and A. Pizzi, Influence of wood grain direction on linear welding. *J. Adhes. Sci. Technol.* **23**, 2047–2055 (2009).
14. C. Ganne-Chedeville, G. Duchanois, A. Pizzi, F. Pichelin, M. Properzi, and J.M. Leban, Wood welded connections: Energy release rate measurement. *J. Adhes. Sci. Technol.* **22**, 169–179 (2008).
15. P. Omrani, H.R. Mansouri, G. Duchanois, and A. Pizzi, Fracture mechanics of linearly welded wood joints: Effect of wood species and grain orientation. *J. Adhes. Sci. Technol.* **23**, 2057–2072 (2009).
16. M. Rhême, J. Botsis, J. Cugnoni, and P. Navi, Influence of the moisture content on the fracture characteristics of welded wood joint. Part 1: Mode I fracture. *Holzforschung* **67**, 747–754 (2013).
17. M. Rhême, J. Botsis, J. Cugnoni, and P. Navi, Influence of the moisture content on the fracture characteristics of welded wood joint. Part 2: Mode II fracture. *Holzforschung* **67**, 755–761 (2013).
18. H. Zhang, A. Pizzi, X. Zhou, X. Lu, and Z. Wang, The study of linear vibrational welding of moso bamboo. *J. Adhes. Sci. Technol.* DOI: 10.1080/01694243.2017.1322767
19. Y. Li, B. Xu, Q. Zhang, and S. Jiang, Present situation and the countermeasure analysis of bamboo timber processing industry in China. *Journal of Forestry Engineering*, **1**, 2–7 (2016).
20. H. Li, Q. Zhang, G. Wu, X. Xiong, and Y.Li, A review on development of laminated bamboo lumber. *Journal of Forestry Engineering*, 1, 10–16 (2016).
21. H.R. Mansouri, P. Omrani, and A. Pizzi, Improving the water resistance of linear vibration-welded wood joints. *J. Adhes. Sci. Technol.* **23**, 63–70 (2009).
22. P. Omrani, A. Pizzi, H.R. Mansouri, J.M. Leban, and L. Delmotte, Physico-chemical causes of the extent of water resistance of linearly welded wood joints. *J. Adhes. Sci. Technol.* **23**, 827–837 (2009).
23. M.I.P. Peña, A.L. Deutschle, B. Saake, A. Pizzi, and F. Pichelin, Study of the solubility and composition of welded wood material at progressive welding times. *Eur. J. Wood Wood Prod.* **74**, 191–201 (2016).